

EVALUATION OF SILICON NITRIDE AS AN ADVANCED RADOME MATERIAL

Various forms of silicon nitride (Si_3N_4) are investigated to determine their suitability as radome materials for hypersonic, radar-guided missiles. The Applied Physics Laboratory has directed test efforts to assess the performance of these materials for use in radome manufacture. A database of thermal transport and mechanical properties has been generated by the developers of these materials and by other independent laboratories. The Laboratory suggested standard surface-finish techniques and a uniform sample size and shape for use by all suppliers so that direct comparisons could be made. The results of tests conducted from 1985 to 1988 on mechanical strength and particle impact damage are presented along with an explanation of the methods for obtaining reliable strength and toughness values essential for radome design.

RADOME DESIGN REQUIREMENTS

All guided missiles depend on electromagnetic (EM) wave sensors to detect energy that is either emitted or reflected from the target. The EM sensors are integrated into a closed-loop tracking system that measures the line of sight (LOS) angle between the missile axis and the target position. Reliable atmospheric intercepts, where closing velocities sometimes exceed 10,000 ft/s, require that the LOS angle measurement be accurate to a fraction of a milliradian. Because it is located at the front of the missile, the EM sensor window must provide a low-drag contour and not interfere with the EM waves. For radar-guided missiles, these fundamental requirements indicate the use of a mechanically strong material that is transparent to microwave energy. This latter requirement means that the window should have a low dielectric constant (also called permittivity) and low EM absorption (called loss tangent). Metal oxides, specifically many polycrystalline ceramics, meet these requirements of high strength and dielectric permittivity.

When naval weapons designers address countering airborne threats to ships at sea, the inevitable conclusion is to increase the flight speed and maneuverability of the defensive missiles. Higher speeds lead directly to higher structural temperatures in the missile, particularly in the radome. Also, high radome temperature will result in diminished strength and an increase in both dielectric constant and loss tangent, either of which can lead to intercept failures. A missile that flies through rain can suffer considerable impact damage, resulting in greatly reduced strength.

Measurements made on small laboratory samples can be used to evaluate the structural suitability of silicon nitride as a radome material. Mechanical load studies of an advanced radome on expected flight trajectories have resulted in an explicit set of thermal and structural radome requirements. The radome considered is a 10° half-angle cone, 14 in. in diameter with a wall 0.125 in. thick. During flight, very rapid boost phases and the ability to pull

100-g lateral turns result in thermal and mechanical stresses that total about 35,000 psi of tension at the inner surface of the radome. Wall temperatures during this loading reach a maximum of about 2200°F. Encounters with rain, ice, or dust at the angle of attack will likely result in impacts at velocities around 8,000 ft/s at angles of 15° to 20° to the surface. A successful advanced radome material such as silicon nitride must endure such loading conditions.

Silicon nitride exists as an ionic bonded crystalline structure that is very hard and retains its strength at temperatures up to at least 1800°F. This intrinsic characteristic exceeds that of commonly used radome materials such as alumina (Al_2O_3), silica (SiO_2), and cordierite (Al_2O_3 , MgO , and SiO_2). Exploiting this very desirable material for use as a radome requires forming and processing the material into axisymmetric shapes with uniformly thick walls. The art of ceramic fabrication involves many nuances that are often painfully learned through trial and error. Most successful processes are proprietary trade secrets owned by individuals or companies. As a forming process varies, so do the properties of the resultant part. Distinguishing between nominally similar variations of silicon nitride without bearing the considerable expense of producing and testing many full-size radomes becomes possible with proper interpretation of tests on small coupons.

PART MANUFACTURING AND TESTING

Table 1 lists all the silicon nitride samples delivered by the contractors and evaluated by APL. Finished radome shapes were successfully produced only by GTE/Wesgo. The Raytheon Co. did the final grinding of these parts. Contract timing requirements made it necessary to use bar and disk samples from GTE that derived from an experimental material and process called AY6. The AY6 material and process were not sufficiently devel-

Table 1. Silicon nitride samples evaluated by APL.

Supplier	Material	Processing	MOR bars (0.25 × 0.125 × 2.5 in.)	No. of disk specimens ^a	Finished radomes ^d	Radome blanks
Ceradyne, Inc.	CER 147Y	Hot-pressed Si ₃ N ₄	160	58 + 10		2
GTE Laboratories	GTE AY6	Slip-cast, dried, and sintered Si ₃ N ₄	120	59 + 10		
General Dynamics	GD-1	Slip-cast dried, and sintered SiAlON	0	3 + 11		
GTE/Wesgo	SNW-1000	Spray-dried, isostatically pressed, and sintered Si ₃ N ₄	60 ^b 8 ^c	2 + 8	2	
GTE/Wesgo	SNW-9000	Spray-dried and isostatically pressed Si ₃ N ₄	120	0 + 14		
Garrett Corp. Airesearch	G-ACC-C	Sintered, reaction-bonded Si ₃ N ₄ , hot isostatically pressed	120	0 + 14		4
Raytheon	Ray	Slip-cast	120	0		

^aNumber of unimpacted and number of impact tests; disks had 2.5-in. diameters and were 0.125 in. thick.

^bBars 0.177 in. × 0.138 in. × 1.97 in.

^cCut from radome nose, 0.10 in. × 0.05 in. × 1.2 in.

^dBlanks indicate that no samples were produced.

oped by the time that subscale radomes were required; therefore, the well-established SNW-1000 material and process were used instead. Thus, GTE had a strength versus temperature database on AY6, but radomes made from SNW-1000. Subsequently, GTE delivered three sets of SNW-1000 bar samples to APL for testing: one set of eight bars cut from the nose section of one of the radomes and two sets of thirty each for modulus of rupture (MOR) evaluation at room temperature and at 2400°F. The data from these tests are included in the discussion that follows.

Finished conical frusta (about 12 in. high with a small-end diameter of about 6 in.) that demonstrated production and finishing capability of hot-pressed thin shells were produced by Ceradyne. No strength or RF tests could be devised for these parts. Several 14-in.-diameter radome blanks were attempted by Ceradyne Co., but the tip sections did not form properly and could not be ground to finished dimension.¹ The Garrett Corp. produced conical frusta and subscale radome blanks in as-fired condition. The Garrett parts were near net shape in terms of thickness, but they were not sufficiently round to allow finish-grinding to the required uniform, axisymmetric thickness; as a result, no tests were conducted on these parts. The Raytheon Co. produced 120 flexural strength samples and then withdrew from further participation. General Dynamics donated a silica-alumina-oxynitride material; the 14 disks they provided were used primarily for evaluation of particle impact.

Although the production of small-coupon samples is insufficient to certify a radome design, properly conducted tests on small coupons can be related via statistical analysis to an eventual full-size radome. Of particular interest here is the measurement of ultimate flexural bend strength versus temperature. All manufacturers were required to produce modulus of rupture bars (0.25 in. wide × 0.125 in. thick × 2.5 in. long) for testing at room temperature, 1800°F, 2200°F, and 2550°F. At each temperature, a set of thirty bars of each material was required.

These tests produced uniaxial bend strength versus temperature for each material and served as an initial screening. Table 2 summarizes these results and includes some statistical parameters (discussed later). A strength test that more closely resembles the loading that radomes experience during flight is the biaxial flexure test, which applies a biaxial bending stress in the central portion of a cylindrical disk via concentric loading rings (Fig. 1). An additional benefit of the biaxial disk test is that, unlike the four-point bar arrangement, no edges or corners are in the highly stressed area of the disk. Groups of thirty disks were produced for tests at room temperature and 2400°F by Ceradyne and GTE/Wesgo. Data from these tests are also presented in Table 2.

Data Analysis

In a collection of N measurements of the stress at failure (σ) of identical samples, it is possible to rank each discrete strength measurement, σ_i , in ascending order. A probability of failure, PF_i , is assigned to each measurement: $PF_i = i/(N + 1)$. According to the Weibull reliability statistic,² data of this type can be represented by the following relationship:

$$\ln[1/(1 - PF)] = \int_S (\sigma / \sigma_0)^m dS, \quad (1)$$

where the subscript i is dropped to denote a continuous distribution of failure probabilities over all stress levels, σ ; σ_0 is a characteristic strength; m (called the Weibull modulus) is related to the dispersion of both the size and location of strength-limiting flaws within the stressed part; and S represents the physical boundary of the test sample under load and can be interpreted as either an area or a volume. For a collection of samples with the same size and stress distribution, the Weibull formula can be linearized as

$$\ln\{\ln[1/(1 - PF)]\} = m \ln \sigma + C_1. \quad (2)$$

Table 2. Strength test results for silicon nitride.

Manufacturer	Average failure strength (1000 psi)	Weibull modulus (m)	Temperature (°F)	No. of samples	Weibull slope coefficient of determination (r^2)
MOR bars					
CER 147Y	101	7.7	RT	30	0.976
	76	5.8	1800	30	0.929
	87	9.5	2200	30	0.965
	50	10.5	2550	30	0.954
Garrett ACC-C	75	6.9	RT	37	0.940
	67	9.3	1800	10	0.969
	44	5.9	2200	10	0.879
	10	5.9	2550	10	0.946
Raytheon	75	7.7	RT	30	0.979
	71	12.1	1800	30	0.952
	41	7.4	2200	30	0.926
	19	7.3	2550	29	0.909
GTE AY6	67	8.4	RT	30	0.951
	63	7.1	1800	30	0.903
	41	9.2	2200	30	0.946
	21	8.5	2550	30	0.850
GTE SNW-1000	100	10.1	RT	30	0.880
	66	15.1	2400	30	0.850
	97	19.6	RT	8 ^a	0.932
CER 147A	90	9.2	RT	10 ^a	0.916
	90	8.6	1800	10 ^a	0.921
	73	10.7	2200	10 ^a	0.913
	47	37.4	2550	10 ^a	0.886
Disks					
CER 147Y	98	12.9	RT	26	0.980
	75	8.4	2400	26	0.980
GTE AY6	55	6.7	RT	30	0.926
	30	8.7	2400	27	0.976
SNW-1000	74		RT	2 ^a	
SNW-9000	57		RT	1 ^a	

Note: MOR = modulus of rupture, RT = room temperature.

^aSample size was too small for high confidence in Weibull modulus.

If the average strength of a collection of samples of modulus of rupture bars is denoted MOR [$MOR = (\sum_{i=1}^N \sigma_i)/N$], then by definition the PF for any sample loaded to that stress level is $PF(MOR) = 0.5$. Alternately, a population of modulus of rupture bars can be produced, only a small percentage of which (i.e., PF_D) fail when loaded to the design stress, σ_D . In either case, values of MOR and m for these bars are given as

$$\ln(MOR) = [\ln(\ln 2) - C_1] / m, \quad (3)$$

where

$$C_1 = \ln \left\{ \ln \left[1 / (1 - PF_D) \right] \right\} - m \ln \sigma_D. \quad (4)$$

Neil³ suggests that this relationship can be used to examine the trade-off between average strength and the scatter or variability of strength data, represented in m : a material with a high average strength and high degree of scatter (low m) will not meet design requirements (σ_D and PF_D)

as well as a material with moderate average strength and very little scatter (high m). This notion is presented in the context of the present radome design requirements in the following paragraphs.

The Weibull statistic provides a guideline for projecting the failure stress of small samples to the failure stress in a radome at equivalent probabilities as

$$\sigma_B / \sigma_R = (S_R / S_B)^{1/m}, \quad (5)$$

where subscripts R and B are for radome and bars, respectively. Alternatively, a radome can be thought of as composed of $N \equiv (S_R / S_B)$ bar elements, each of which must have a probability of survival, PS_n , at the radome design stress such that the radome failure probability, PF_R , is

$$1 - PF_R = \prod_{n=1}^N PS_n \approx PS_B^N, \quad (6)$$

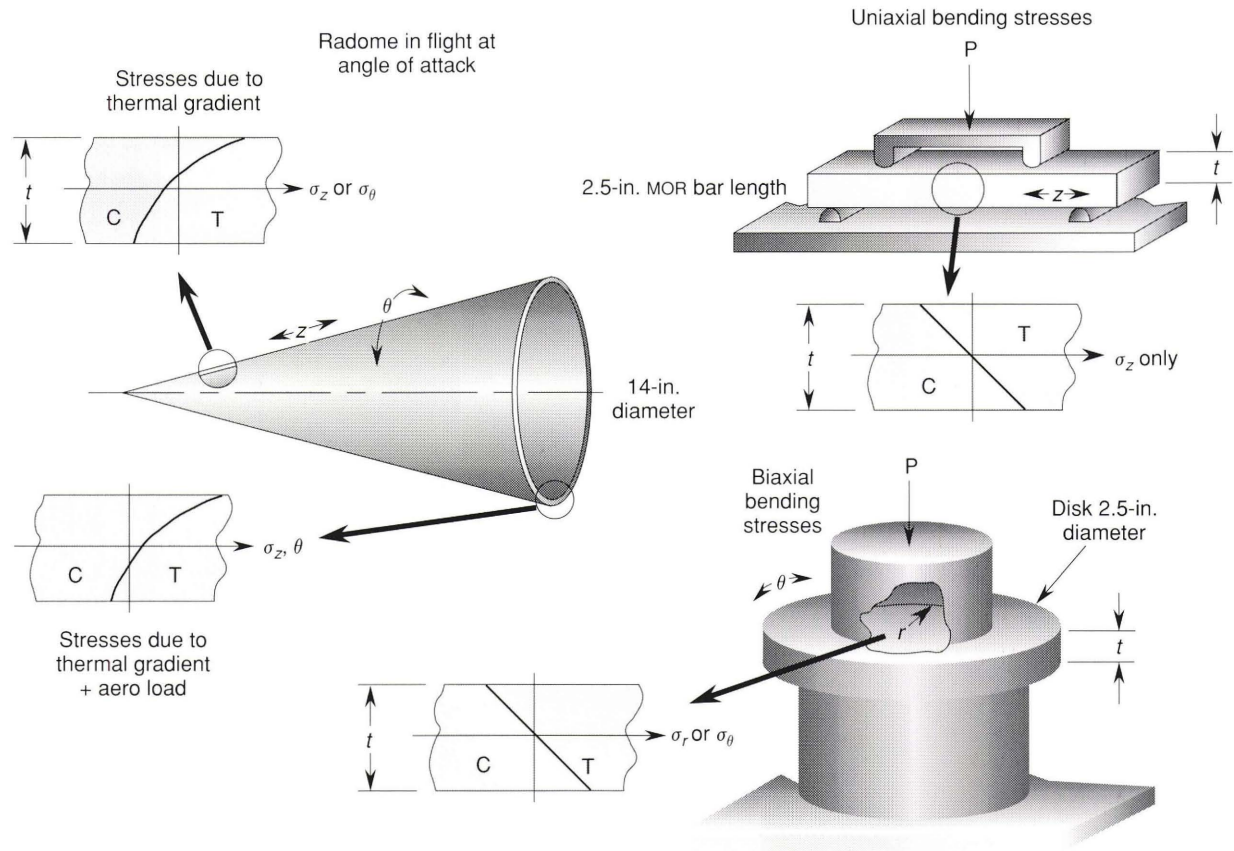


Figure 1. Stress distributions in radomes and flexural strength samples. C = compression, T = tension, P = test load; t = thickness ≈ 0.125 in.; MOR = modulus of rupture; r , z , and θ = local coordinate directions.

where PS_B is the required probability of survival of a collection of modulus of rupture bars loaded to the radome design stress. The equality holds only to the extent that stress distributions in the modulus of rupture bars and radome elements are equal. The small biaxial disk samples tested here conform to this requirement as much as possible.

Equation 5 can be used with Equations 3 and 4 to define the modulus of rupture for bars at equivalent failure rates, or Equation 6 can be used with Equations 3 and 4 to identify the minimum acceptable failure probability rate in bars loaded to the radome design stress. Figures 2 to 4 illustrate this comparison for the present radome design stress of 35,000 psi and several radome failure probabilities between 5% and 0.01%. The size ratios consider the relative stressed volumes of bars, disks, and the radome.

The modulus of rupture bar and flexural disk data listed in Table 2 are plotted in Figures 2 to 4 to show the relative merit of the different materials as radome candidates. In evaluating these data, the area above and to the right of a given failure probability curve represents acceptable performance, whereas the area below and to the left of the curve represents an excessive probability of failure. Note that the slight difference among the requirements curves for a given probability of failure reflects the different volume ratios of the radome and the

respective strength samples. Also, the data for room temperature and elevated temperature are plotted together, although the radome design condition is actually for the high-temperature condition. These design curves show that the requirements are beyond, or possibly just at, the state of the art for these ceramics. The GTE/Wesgo SNW-1000 material most nearly meets the design conditions as stated here; however, this conclusion is based on modulus of rupture bar strength data only, as no biaxial flexure disks of SNW-1000 were made.

A fundamental assumption made in the foregoing discussion and in constructing Figures 2 to 4 is that the mechanisms for failure, the distribution and types of flaws, and the stress distributions present in radomes and small strength samples are identical. The latter assumption is obviously not correct insofar as the radome stresses are a result of a combination of biaxial thermal bending in an axisymmetric shell superimposed on either tension or compression due to aerodynamic maneuver loads. The modulus of rupture bars experience unidirectional bending stresses, and the disk samples have biaxial bending. These differences are illustrated generically in Figure 1. The assumption of equal stress distributions among sample groups can be relaxed by a more rigorous evaluation of the Weibull integral (see Ref. 4 for details).

The starting powders, forming techniques, firing schedules, and grinding operations used to produce ra-

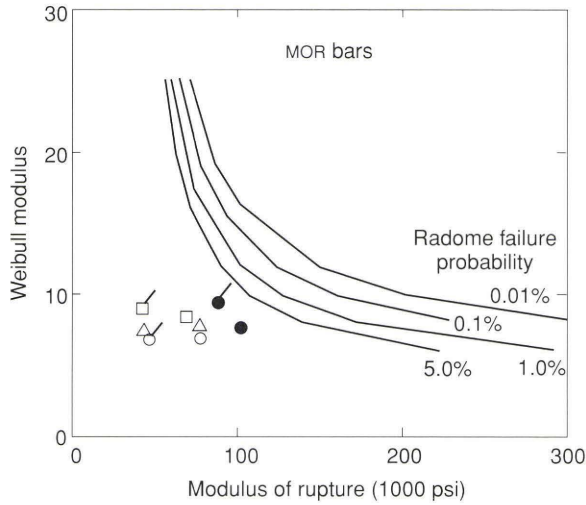


Figure 2. Modulus of rupture bar strength requirements for a design stress of 35,000 psi and size ratio of 4660. Flagged symbols = 2200°F; unflagged symbols = room temperature, ● = CER 147Y, □ = GTE AY6, △ = Raytheon, ○ = Garrett.

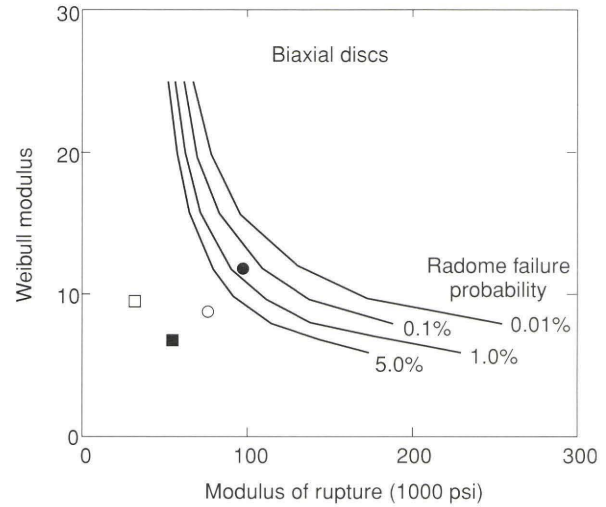


Figure 4. Biaxial disk flexure strength requirements for a design stress of 35,000 psi and size ratio of 1110. Filled symbols = room temperature, open symbols = 2400°F, ○ = CER 147Y, □ = GTE AY6.

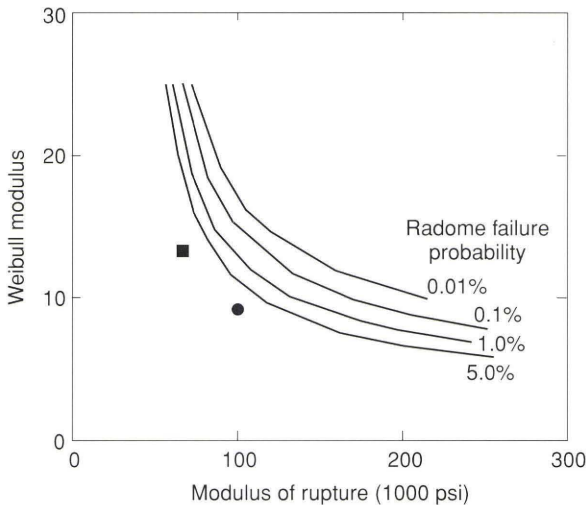


Figure 3. Modulus of rupture bar strength requirements for a design stress of 35,000 psi and size ratio of 11,000 for SNW-1000. ● = room temperature, ■ = 2400°F.

domes and strength samples will certainly vary among manufacturers and perhaps even within a particular material. All such variations can significantly alter the size and distribution of the strength-limiting flaws, and hence the Weibull statistics. Variations of this type within a sample group are reflected in the degree to which the measured strength values fit the Weibull formula (Eq. 2). Table 2 lists the coefficient of determination (r^2) for all the data groups, generally above 0.90.

PARTICLE IMPACT TESTS

Flat disk samples were impacted with nylon beads shot from an exploding wire apparatus at velocities of approximately 8,000 ft/s. Adler⁵ has shown that for velocities between 4,000 ft/s and 16,000 ft/s, nylon bead impacts cause damage similar to that caused by water drops. For

these tests, beads with a 1.98-mm diameter and 4.7-mg mass were used. The impact angle was 17.5° (90° is normal impact). Tests were conducted with some specimens at room temperature and some at 2400°F. The particle velocity, impact angle, and elevated temperature were selected to be representative of conditions that would be experienced by a radome in flight. After impact, the specimens were subjected to a biaxial flexure test to evaluate their residual strength by Southern Research Institute, which also performed biaxial flexure tests on unimpacted samples; thus, the loss in strength from impact damage could be determined by comparing the biaxial flexure strength of the impacted and unimpacted samples. At General Research Corp., the specimens were measured, weighed, and inspected both visually and with an optical microscope to ensure that the region to be impacted was free of gross flaws.

For the room temperature tests, the samples were placed in a polyethylene holder that provided support around the outer 0.125 in. of the back face of the disks. During the elevated temperature tests, each specimen was held at a 17.5° angle in a graphite oven that was heated inductively. The specimen was heated gradually (for 20 min) to the desired temperature, which was measured by optical pyrometers, and then impacted and allowed to cool slowly to room temperature.

The biaxial flexure tests were conducted using a ring-on-ring test apparatus (Fig. 1). All the biaxial flexure tests of impacted specimens were done at room temperature to avoid subjecting the specimens to several heating and cooling cycles. The impacted samples were placed in the test fixture so that the impact surfaces were in tension.

Because the number of specimens of each material was limited, the following tests of each material were made: a single impact at room temperature on each of three samples, a single impact at 2400°F on each of three samples, and a triple impact at room temperature on each of three samples. When a set of samples numbered more

than nine, they were reserved, first in the event that a test had to be repeated and then for measuring unimpacted strength. The triple-impact tests involved three sequential bead shots aimed at the same location on the sample. In practice, the three impact points did not coincide, but they were quite close.

The results of the impact and residual strength tests are discussed in detail in Ref. 6. A comparison of the average room temperature biaxial flexure strength for unimpacted and impacted samples is presented in Table 3. No biaxial flexure tests were done on unimpacted samples of the Garrett material because not enough of these samples were produced.

CONCLUSIONS

The Ceradyne hot-pressed silicon nitride has the highest strength of all small-coupon samples tested at both high and ambient temperatures. After several attempts, Ceradyne was unable to overcome the difficulties in hot-press forming of the closed-tip section of the radome. No finished radome shapes were produced; therefore, the CER 147Y material is still regarded as experimental for radome applications. No RF measurements, other than dielectric constant and loss tangent, were made.⁷ Flaws resulting from hypersonic particle impact reduce the strength of the Ceradyne material by 30 to 40%.

The Garrett near-net-shape process is very close to making acceptable radome shapes. The several blanks they produced have a generally uniform thickness that is within about 0.060 in. of the required finished dimensions; however, the wall contour is distorted fore to aft and around the circumference too much to allow final grinding. No RF measurements were made on these sub-scale radome blanks. The Garrett coupon samples had the lowest strength characteristics and appear to suffer from excessively large flaws.

The two GTE/Wesgo radomes were delivered on time and finish-ground to the required uniform thickness by Raytheon. These radomes have good Ka-band radar performance at room temperature. Limited RF testing at temperatures around 1800°F shows that RF performance degradation can be partly compensated by an adjustment in radar frequency. No RF measurements at the highest required operating temperature (2800°F) have yet been made. Although very few unimpacted biaxial disk samples of SNW-1000 were tested, the 60 modulus of rupture

bars tested by Southern Research Institute indicate a strength and reliability equal to the Ceradyne hot-pressed material. Although small in both number and physical dimension, the eight bars cut from the finished radome show excellent strength. The residual strengths of the SNW-1000 and Ceradyne materials after particle impact are similar.

All materials undergo a decline in strength from impact damage. Close multiple impacts cause a greater loss of strength than single impacts. The Ceradyne material has the highest unimpacted strength so that, even though the strength decreases by 28.8% after a single impact, it still has the highest strength of all the single-impact materials. After three impacts, the Ceradyne strength is below, but comparable to, that of SNW-1000, which has the highest residual strength after three impacts. The strength degrades significantly after one impact, but little further strength reduction is caused by the two additional impacts. These results are based on a very small number of impact tests for each material, so the confidence level in the amount of degradation is not high, and the Weibull moduli cannot be calculated reliably. At the average residual strengths measured here, a Weibull modulus of over 20 would be required to meet the present design goals. Adler⁵ reported microscopic observation of the impact sites:

...the Ceradyne materials exhibited the least amount of crack penetration: on the order of 5% of the specimen thickness. The SNW materials have crack penetration depths that range from 15% to 30% of the specimen thickness. The SNW-1000 materials have consistently deeper cracks than the SNW-9000 materials. From the limited number of crack depth measurements the Ceradyne material has the highest particle impact fracture resistance by a factor of 3 or 4. The next most resistant material is the SNW-9000 followed by SNW-1000.⁵

In summary, the SNW-1000 and Ceradyne 147Y materials demonstrate very similar strengths both before and after hypersonic impacts. These materials are clearly superior to all the others tested here, but they remain slightly below the radome performance requirements. The demonstrated capability for radome production by GTE/Wesgo singles out the SNW-1000 material as the one currently best suited for prototype development. As new

Table 3. Biaxial flexure strengths at room temperature.

Material designation	Average unimpacted strength ^a (no. of samples)	Average single impact ^a (no. of samples)	Decrease in strength (%)	Average triple impact ^a (no. of samples)	Decrease in strength (%)
GD-1	15,000 (3)	6,540 ^b (3)	56	6,080 ^c (1)	59
GTE AY6	54,300 (30)	50,680 (3)	7	43,750 (1)	19
CER 147Y	95,500 (30)	68,010 (3)	29	58,510 (3)	39
SNW-1000	78,120 (1)	62,240 (3)	20	59,800 (3)	23
SNW-9000	57,320 (1)	57,183 (3)	0.2	45,055 (2)	21
G-ACC-C	NA	51,462 (3)	NA	46,653 (5)	NA

Note: NA = not analyzed.

^aMeasured in psi.

^bThis value is for the onset of fracture, but the strength at complete failure was much higher.

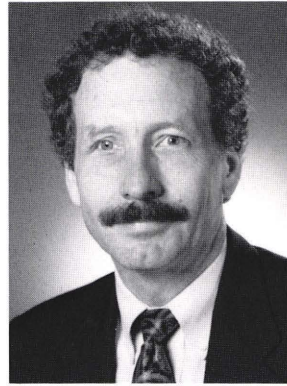
^cThe flexural strength after two impacts. A third impact would result in the complete fracture of the specimen; the flexural strength would be zero.

materials are developed with improved fracture toughness and higher temperature capability, the evaluation methods described here, using carefully controlled tests on small coupons, can be applied to obtain reliable radome design values for strength and resistance to rain damage.

REFERENCES

- ¹Negrych, J. A., *Fabrication of Hot Pressed Silicon Nitride Radome/Antenna Windows*, Report No. 83320-22, Ceradyne Inc., Santa Ana, Calif. (1986).
- ²Weibull, W. A., "A Statistical Distribution Function of Wide Applicability," *J. Appl. Mech.* **18**, 293-297 (1951).
- ³Neil, J., "Comments on Strength/Weibull Modulus Tradeoffs for Ceramics," Memo, GTE Labs Inc., Belmont, Calif. (14 May 1987).
- ⁴Strobel, F. A., and Pritchett, L. J., *Statistical Fracture Analysis for Ceramic Radomes*, Final Report No. 86-15/ATD, Acurex Aerotherm Division, Huntsville, Ala. (1986).
- ⁵Adler, W. F., *Surface Launched Weaponry Materials Technology (SURFMAT) Program. Single Particle Impact Testing of Silica Materials*, Final Report, Contract N60921-82-C0207, General Research Corp., Santa Barbara, Calif. (1984).
- ⁶Adler, W. F., *Evaluation of the Particle Impact Resistance of Advanced Radome Materials*, Report No. CR-87-1003, General Research Corp., Santa Barbara, Calif. (1987).
- ⁷Ho, W., and Harker, A. B., "Millimeter Wave Dielectric Properties of Radome and Window Materials," in *Proc. 1st DoD E-M Windows Symposium*, Naval Surface Weapons Center, White Oak, Md. (15 October 1985).

THE AUTHOR



R. KELLY FRAZER earned B.S. and M.S. degrees in mechanical engineering from Carnegie Institute of Technology in 1966 and 1968, respectively. Mr. Frazer was employed by APL in the Aeronautics Department as a summer student in 1966 and 1967 and joined the Associate Staff in November 1967. He was appointed to the Senior Staff in 1979 and to the Principal Staff in 1990. Mr. Frazer has worked on radome thermal and mechanical analysis as well as testing throughout his career at APL. Other assignments have included thermal analysis of the

Tomahawk cruise missile guidance set, thermal management of electronics boards aboard the Hopkins Ultraviolet Telescope, and modeling of temperatures in the inner ear during caloric testing for vestibular function. Mr. Frazer is currently section supervisor of the Thermal Analysis Section.